Importance of the Annual Cycles of SST and Solar Irradiance for Circulation and Rainfall: A Climate Model Simulation Study

Y. C. Sud, G. K. Walker[@], V. M. Mehta[&]
and
William K.-M. Lau

ABSTRACT

Annual cycle of climate and precipitation is related to annual cycle of sunshine and sea-surface temperatures. Understanding its behavior is important for the welfare of humans worldwide. For example, failure of Asian monsoons can cause widespread famine and grave economic disaster in the subtropical regions. For centuries, meteorologists have struggled to understand the importance of the summer sunshine and associated heating and the annual cycle of sea-surface temperatures (SSTs) on rainfall in the subtropics. Because the solar income is pretty steady from year to year, while SSTs depict large interannual variability as consequence of the variability of ocean dynamics, the influence of SSTs on the monsoons are better understood through observational and modeling studies whereas the relationship of annual rainfall to sunshine remains elusive. However, using NASA's state of the art climate model(s) that can generate realistic climate in a computer simulation, one can answer such questions. We asked the question: if there was no annual cycle of the sunshine (and its

associated land–heating) or the SST and its associated influence on global circulation, what will happen to the annual cycle of monsoon rains. By comparing the simulation of a 4–year integration of a baseline Control case with two parallel anomaly experiments: i) with annual mean solar and ii) with annual mean sea–surface temperatures, we were able to draw the following conclusions:

1. Tropical convergence zone and rainfall which moves with the Sun into the northern and southern hemispheres, specifically over the Indian, African, South American and Australian regions, is strongly modulated by the annual cycles of SSTs as well as solar forcings. The influence of the annual cycle of solar heating over land, however, is much stronger than the corresponding SST influence for almost all regions, particularly the subtropics.

2. The seasonal circulation patterns over the vast land–masses of the Northern Hemisphere at mid and high latitudes also get strongly influenced by the annual cycles of solar heating. The SST influence is largely limited to the oceanic regions of these latitudes.

3. The annual mode of precipitation over Amazonia has an equatorial regime revealing a maxima in the month of March associated with SST, and another maxima in the month of January associated with the solar annual cycles, respectively. The baseline simulation, which has both annual cycles, depicts both annual modes and its rainfall is virtually equal to the sum of those two modes.

4. Rainfall over Sahelian–Africa is significantly reduced (increased) in simulations lacking (invoking) solar irradiation with (without) the annual cycle. In fact, the dominant influence of solar irradiation emerges in almost all monsoonal–land regions: India, Southeast Asia, as well as Australia. The only exception is the Continental United States, where solar annual cycle shows only a relatively minor influence on the annual mode of rainfall.

Importance of the Annual Cycles of SST and Solar Irradiance for Circulation and Rainfall: A Climate Model Simulation Study.

Y. C. Sud, G. K. Walker@ ,V. M. Mehta&

and

William K.-M. Lau

Climate and Radiation Branch

Laboratory for Atmospheres

NASA/GSFC Greenbelt, MD 20771

ABSTRACT

A version of the GEOS 2 GCM, which contains new upgrades to the model's prognostic clouds, cloud microphysics, and snow and ice hydrology was used to isolate the influences of the annual cycles of solar irradiation and sea-surface temperatures (SSTs). Four 50-month long integrations were produced with the GCM. The first integration, called Control Case C, used daily interpolated SSTs from a 30-year climatology of monthly SST; the incoming solar irradiation was calculated normally, i.e., at hourly intervals, in this simulation. Consequently, both SSTs and incoming solar irradiance had their natural annual cycles. The two anomaly experiments used i) annual mean prescribed incoming solar called S1 and ii) annual mean SST, called S2, whereas everything else was kept similar to C. In the fourth integration, both SSTs and incoming solar fluxes at the top of the atmosphere were maintained at annual mean values. This constraint virtually eliminated the entire annual cycle forcing of the simulated earth-atmospheric system. *An intercomparison of these simulations revealed the following:*

1. The northward excursions of the monsoon rainfall, specifically over the Indian and Australian regions are strongly modulated by the annual cycles of SSTs and solar forcings. Relatively, the influence of the annual cycle of solar heating over land is stronger than SST forcing for almost all regions, particularly the tropics.

2. The rainfall and circulation patterns over the Kuroshio currents region off the East Coast of Asia are strongly linked to the annual cycle of SSTs.

3. The seasonal circulation patterns over the vast land-masses of the Northern Hemisphere at mid and high latitudes get strongly influenced by annual cycle of solar heating.

4. The annual mode of precipitation over Amazonia has an equatorial regime revealing maxima in March in the S1 simulation; and maxima in January in the S2 simulation. Case C, which has both annual cycles, depicts both annual modes of rainfall. Over South America, the annual mode in C is roughly equal to the sum of the annual modes for SST and solar annual cycles, in S1 and S2, simulations. Annual mode of C is a linear sum of solar and SST forcings.

5. Rainfall over Sahelian Africa is significantly reduced (increased) in simulations lacking (invoking) solar irradiation of with (without) the annual cycle. In fact, the dominant influence of solar irradiation emerges in almost all monsoonal-land regions: India, Southeast Asia, as well as Australia. The only exception is the Continental United States, where solar annual cycle shows only a relatively minor influence on the annual mode of rainfall.

6. The simulated 30-60 day oscillations (or TIOs) were reasonably robust in each of the four simulations. It suggests that TIOs are an outcome of the internal dynamics of the atmosphere that may in turn be forced by the interactions among the physical processes. Nevertheless, simulated TIOs are not materially affected by the annual cycle of SST or solar forcing. This conclusion is also borne out by the robustness of the observed TIO-modes through out the year.

1. Introduction

It is common knowledge that solar irradiance drives all biogeophysical processes on the Earth and dynamics of the earth-atmosphere system. However, the emitted solar irradiance reaching the Earth is essentially constant over time (varies by less than 0.1%) whereas the Sun's declination varies hugely over an annual cycle and is responsible for large variations in the annual cycle of solar energy income at different latitudes. This in turn leads to a multitude of inter-related annual cycles of our environment. These annual cycles are modulated by three major heat and moisture reservoirs of the Earth-atmosphere system, namely atmosphere, oceans, and land. These reservoirs absorb selectively the incoming solar fluxes and turn them into thermal energy. The thermal energy, with diurnal and/or annual time lag, can appear either at the same location (as in the case of land), or emerges at a variety of locations due to hydrodynamic transports within the reservoir (as is the case for oceans and the atmosphere). The latter exhibits a much more complex time-lag structure, which could vary hugely- anywhere from a few hours to an entire season and longer, even decades and centuries. These in turn introduce a variety of complexities in the annual cycles of climate. Naturally therefore, annual cycle of solar irradiance is the primary cause of the entire internal dynamics within each reservoir, imparts a variety of time scales in the forcing of different areas of the Earth-Atmosphere system, and hugely complicates the outcome because of nonlinear interactions among them.

There is a vast body of literature on the influence of the SSTs and the solar heating of Eurasian landmasses (e.g., Tibetan Plateau) and on the ensuing tropical circulation and Asian African and Australian monsoons (e.g., Krishnamurti and Kishtawal., 2000). Studies by Gadgil (2000), Kitoh and Noda (1999), Torrence and Webster (1999), Lau and Wu (1999) and Chandrasekar and Kitoh (1998) discuss several aspects of these interactions vis-a-vis Asian Monsoons. Historically, some have viewed monsoons to be a gigantic sea breeze arising from the thermal contrast among Eurasian land-masses and tropical SSTs (Webster et al., 1998). Others have argued that monsoons are associated with the location of the Inter Tropical Convergence Zone (ITCZ) and the related outflow into the Rossby waves (Chao et al., in review). More recently, some view the Tropical Intraseasonal Oscillations (TIOs) with the associated northward propagation as the primary modulator of monsoon variations (Lau and Chan, 1988). In fact a version of the GLA GCM with a reasonable representation of TIO-modes also captured the Indian monsoon variability reasonably well in AMIP-I simulations (Yang and Lau, 1998; and Gadgil and Sajani, 1998). For these reasons, there is considerable uncertainty about how physical processes and/or surface forcings influence the tropical circulation, specifically the propagation of monsoons into higher latitudes.

The most dominant component of the external physical forcing of the Asian Monsoons is the atmospheric annual cycle (and its dynamical consequences). The annual cycle manifests in all biogeophysical processes that affect the terrestrial biosphere, sea surface temperatures (SSTs), as well as the weather and climate on Earth. Notwithstanding the importance of the interannual variations of the dynamical climate, such as forced by SSTs, for example, through the well-known El Nino / La Nina episodes, we shall focus primarily on the understanding of the annual cycle. The goal is to discern the relative influences of solar forcing on atmospheric circulation and dynamics through a short (long) response time-scale of land (ocean). An understanding of the response of the climate system to the solar and SST annual cycles would potentially decipher the complexities of the stationary and transient variations of the annual cycle of climate. *Such considerations have provided the primary motivation for the investigation reported in this paper.*

GCMs have been used extensively for simulating the influence of the external boundary forcings on the development of future weather and climate (seasonal means), hydrologic processes,

precipitation and its interannual variability (see, e.g., IPCC Reports I, 1990 and II, 1995). We propose to examine the influence of the annual cycle related changes in surface fluxes at the land-atmosphere and ocean-atmosphere interfaces on the annual mode of climate using a state-of-the-art General Circulation Model (GCM). We isolate these influences by suppressing the solar and/or SST annual cycles in otherwise similar sets of simulations. The key requirement as well as the limitation of such an investigation is reliance on a GCM; consequently, the chosen GCM must be sufficiently credible to realistically respond to the prescribed changes in external forcings. The climate version of GEOS 2 (Goddard Earth Observing System, version 2) GCM fulfills these requirements. Indeed, in view of the useful research and several ongoing upgrades (discussed in section 2) to the physical parameterizations of the GCM, the current version, 4-deg. X 5-deg. (horizontal resolution) X 20-sigma layers (vertical resolution), of the GEOS 2 GCM is particularly suitable for the proposed investigation. The only other requirement is to find a way to prescribe the annual mean SSTs (from the analysis of observations) and the annual mean solar forcing at the top of the atmosphere. Both of them were accomplished quite easily as described in Section 3.

For many problems, particularly those that critically depend upon changes of a few W m^{-2} in external forcing of the atmosphere, the intrinsic limitations of a GCM and the random variability of the climate system can interfere with the statistical data analysis and affect the confidence level of the findings. In other cases, such as Amazonian deforestation studies (e.g., Hahmann and Dickinson, 1997), the disagreement among GCMs in the simulated climate scenarios have raised some concerns causing some key questions to remain unresolved. Therefore, one must ascertain that any GCM used for a specific study be suitable for it. Nevertheless, one would like to eventually reaffirm these findings with other state-of-the-art GCMs. Shukla and Fennessy (1994) used the COLA GCM to perform a similar, though not identical, simulation study in which the solar radiation and/or the SSTs were held constant at equinox values in subsequent Boreal Spring and Summer simulations. The documented version of their results (personal communication M. Fennessy, 2000) primarily focused on the Indian monsoon. Our paper endeavors to discern the influence of the annual cycle of SSTs and solar forcing on the annual cycles of entire global circulation and rainfall. We will show that the Indian-monsoon related findings basically agree with Shukla and Fennessy (1994); however, our diagnostics are broad based because we also examine several global-scale consequences of the solar and SST annual cycles. To the best of our knowledge, these influences of solar and SST annual cycles have not been examined in this fashion in previous modeling studies. The rest of the paper is divided into the following four sections. Model description is given in section 2, design of the simulation experiments in summarized in section 3; key results are shown in section 4; discussion of our results and conclusion are provided in section 5.

2. General Circulation Model

The GEOS 2 GCM is a grid-point model and employs a staggered Arakawa C-grid using Version 2 of the Aries/GEOS Dynamical Core for its finite difference algorithm. This algorithm invokes a fourth-order energy and enstrophy conserving scheme, which has been generalized for a non-uniform grid on the spherical Earth (Suarez and Takacs, 1995). In the physics package, the model uses Helfand and Labraga (1988) turbulent closure, Zhou et al. (1996) gravity wave drag, and new upgrades to land-surface and cloud-dynamical and microphysical, processes. Our version has two recent additions that are significant. One is the prognostic cloud-radiative forcing (CRF)

invoked through the use of McRAS (Sud and Walker, 1999; discussed in section 2.1). This upgrade is particularly relevant for assessing the influence of interactive clouds (Del Genio et al., 1996). The second important upgrade is in the surface hydrology, specifically the influence of snow/ice process on land. The other upgrades of GEOS 2 GCMs are the features such as (i) ability to perform coordinate translation and rotation with a provison for relocating the mathematical poles to any arbitrary location (irrelevant for this investigation); and (ii) the fractional cloudiness and cloud optical properties.

2.1 Cloud Physics: McRAS

Microphysics of clouds with Relaxed Arakawa-Schubert Scheme (McRAS; Sud and Walker, 1999a) explicitly provides for three types of clouds- convective, stratiform, and boundary layer. These clouds co-exist and have simultaneous life cycles invoking condensation, cloud generation and dissipation, and precipitation production. We briefly summarize different elementary modules of McRAS.

Relaxed Arakawa-Schubert Scheme (RAS) due to Moorthi and Suarez (1992) is the moist convection of McRAS. It uses a 10-m adjustment time-step with an assumed relaxation time-scale of 1-h. The location of the convective cloud base is diagnosed to be the top of the nearest layer from the surface of the Earth in which the Relative Humidity (RH) exceeds 90% of the critical relative humidity, RH_{crit} of the large-scale clouds. This search is limited to the four near-surface levels, however. The buoyancy to carry the convective mass flux (with associated precipitation loading and momentum dissipation) to its detraining level is provided by the thermal energy of moist convection through the Critical cloud work function (CCWF). Moist convection causes supersaturation, in-cloud condensation, which generates cloud water and fractional cloud cover using cloud microphysics of McRAS.

Stratiform clouds can form if the grid average layer RH exceeds RH_{crit} (Slingo, 1987). There are three scenarios: supersaturated RH, and RH more (or less) than the RH needed to maintain the existing clouds. Each is handled differently. In-cloud RH must always be maintained at 100%. If in-cloud RH drops below 100%, some cloud water must be evaporated adiabatically to raise RH back to 100%. If the available cloud water is insufficient to maintain 100% RH, all cloud water evaporates and the entire cloud mass vanishes. Further details of these features of our cloud physics are discussed in Sud and Walker, (1999a).

The boundary layer (BL) clouds are produced when the BL convection (which generally commences as dry convection) enables BL eddies to become supersaturated at or before the detrainment level where-at cloud buoyancy is neutral. The cloudy air is deposited at the detrainment level. These eddies naturally provide BL clouds an ability to deposit any water vapor content (often more) into the detraining environment than its surroundings -- a typical configuration of counter gradient fluxes.

Conversion of condensate into precipitation follows Sundqvist (1988; 1989). There is no special treatment for ice-phase beyond the implicit adjustment of the time-scales and the empirical constants, and saturation vapor pressure for the ice phase. Full cloud microphysics remains active at all times, affecting all cloud condensate including the cumulus towers and anvils. Clouds in McRAS convect, diffuse, and advect both horizontally and vertically. Again cumulus tower debris

can produce grid-scale cloudiness and humidification regardless of the RH of the host/detraining layer.

The cloud destruction mechanisms are the same for all clouds. They include: (i) diffusion of dry air into the cloud at subgrid scale called cloud munching; (ii) evaporation of in-cloud water through convective scale subsidence and associated adiabatic warming; (iii) cloud top entrainment instability (CTEI) among adjacent cloudy and clear layers (Del Genio et al., 1996); and (iv) cloud-mergers including entrainment of ambient clouds into convective towers and downdrafts.

2.2 Convective Downdrafts

The convective downdrafts and rain-evaporation follow Sud and Walker (1993). It has been variously shown that convective downdrafts can have a significant influence on the simulation (e.g., Mandke et al., 1999). The precipitation falling inside cumulus towers (assumed saturated) does not evaporate. However, all the anvil precipitation, and some of the tower precipitation that emerges into the unsaturated environment, as a consequence of tilting of the convective tower, evaporates and could produce downdrafts if the excess negative buoyancy production criteria of Sud and walker (1993) were satisfied. Downdrafts entrain ambient air and cloud water, which evaporates instantaneously because of the size of cloud water droplets. In addition, the tower precipitation, emerging beneath the cloud base, often satisfies the excess negative buoyancy criteria and leads to downdrafts. The statistical distribution of hydrometeors in idealized cloud geometry follows Del Genio et al. (1996) for water clouds and Ou and Liou (1996) for ice clouds. For more details refer to Sud and Walker (1999, Part I).

2.3 Land Model

Our basic land model is Simple SiB (SSiB) due to Xue et al (1991). This model has been tested with several datasets, but land models of the present day need to be constantly evaluated and improved, often region by region. A brief discussion of several improvements to the land model can be found in Mocko and Sud (2001). One also notices that SSiB parameterizes inter-layer hydraulic conduction among its layers invoking Richard's Equation with several assumptions help to simulate reasonable vertical fluxes. Indeed, lack of subgrid scale variability is an outstanding limitation of the current SSiB, but that is a separate issue and we must postpone its treatment for a later time. SSiB was also evaluated with ISLSCP Initiative I data under GSWP (Dirmeyer et al, 1999) as well as against other simple land schemes (Mocko and Sud, 1998). Only 10 different biomes and soil types are currently allowed in SSiB; yet another restriction is - any single grid cell is allowed to maintain only one soil type and one biome. In other words, tiling is not feasible in the current design. However, grid-scale variability can be introduced by allowing full flexibility in the choice of fractional vegetation covers and leaf area indices.

2.4 Radiative Transfer

McRAS is designed to perform cloud radiative forcing in a fully interactive dynamical framework. It provides cloud mass fraction, cloud droplet and/or cloud ice crystal path lengths, and effective radii of cloud particles. The in-cloud water and ice mass fractions are diagnosed. One modification is in the calculation of equivalent plane-parallel optical thickness using Cahalan (1994) correction for cloud water inhomogeneity. The second modification is in the diagnosed number density and effective radius of ice clouds as a function of temperature following Lohmann et al. (1998). The

structure of this distribution for an arbitrary in-cloud water substance is shown in Sud and Walker (1999a).

There are 4-bands in the shortwave (Chou et al., 1998 a) and 9-bands in the longwave (Chou et al., 1998 b) radiation. For each band, we require the optical thickness, single scattering albedo, and asymmetry factor, for the clouds (see Sud and Walker, 1999a Table 2 for optical parameters). The linearized approximations to the precise radiative transfer equations are given in Chou et al. (1994).

The optical thickness, single scattering albedo, and asymmetry factor for in-cloud water and ice mixtures employ a weighted summation.

The clouds in any atmospheric column are divided into three height groups. Within each group, the clouds are assumed to be maximally overlapped while amongst different groups, they are assumed to be randomly overlapped. For optical thickness of different clouds within the group, smaller clouds are smeared to the size of the largest cloud of the group; this entails adjustment of the in-cloud optical thickness for each cloud except the largest. The specific calculation differs somewhat for shortwave and longwave radiation.

For longwave radiation, the effect of back scattering is folded into the emission of an atmospheric layer, and absorption between the levels is calculated by scaling the cloud optical thickness appropriately. With these approximations, the longwave radiative transfer equations for cloudy atmosphere are identical to that for the clear atmosphere. More details can be found in Chou et al. (1998 a & b)

3. Design of the Experiment.

To isolate the influence of the annual cycles of the solar income and the sea-surface temperatures on the global circulation, we produced four 50-month long simulations with the GEOS 2 GCM (Table 1). In the Control case, C, the solar forcing at the top of the atmosphere was calculated hourly while the sea surface temperatures (SST) were interpolated from SST analysis averaged for 30 years; thus the usual annual and diurnal heating cycles are built into the model including the SST and solar income. This choice makes a comparison of model simulation with observations impossible, but there are a large number of model validation studies (e.g., Sud and walker, 1999b) that can be used as a justification in support of the credibility of the GEOS 2 model. On the positive side, however, climatological SSTs eliminates all extraneous interactions except the annual cycle of SSTs.

The Control, C, simulation was complemented by three companion integrations. In the first integration, called S1, the annual cycle of the solar heating was removed, while the SST annual cycle was still intact and was identical to the Control. The monthly zonal solar energy at the top of the atmosphere (Fig. 1) is shown in the left panel; in addition, there are three time-mean solar-income lines on the right panel: Boreal summer (JJA, red line), Boreal winter (DJF, yellow line) and annual-mean (blue line). Such an average solar income was used for the solar influx at the top of the atmosphere. For the second integration called S2, the annual cycle of SSTs was obtained by generating a 12-monthly average of the 30-year SST climatology. Its annual mean was used to drive one annual value for each grid point (Fig. 2); this was prescribed to the GCM for S2

simulation while solar cycle was maintained identical to that of C.

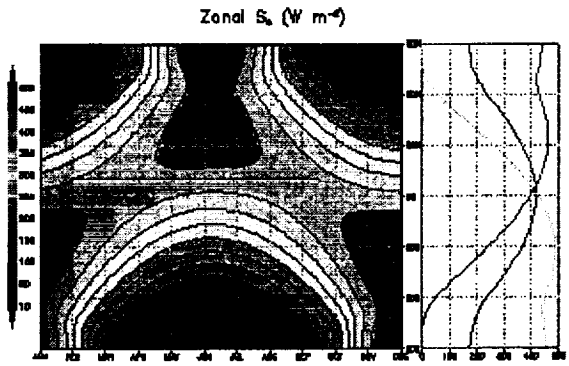

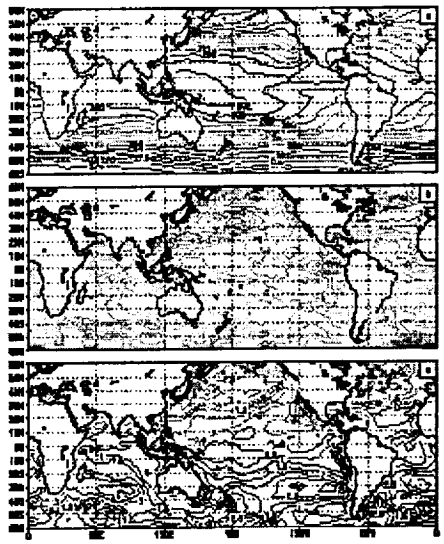

When SST annual cycle is removed, daily interpolation of SST became unnecessary. Indeed, if changes in SST patterns generate anomalous cloudiness patterns, those would clearly interact with the solar and long wave transmissions. In the last integration called S3, the annual mean solar S1 and the annual mean SSTs of S2 were assumed. Consequently, there is no annual cycle forcing in this integration and we do not expect to see any annual cycle after the usual adjustment period. One might ask the question: how does annual mean solar compare with fixing the Sun at the equator (like Shukla and Fennessy, 1992)? We argue that a persistent imbalance in the annual cycle of solar heating over a 50 month long period, such as used here, is likely to cause some violence to the soil moistures anomalies. In other words, it may produce some regions with excessive drying while other may stay too wet and together they might sacrifice the sanctity of the hydrologic processes.

All our simulations started from analyzed initial condition for January 1, 1987. The Control plus three additional simulations (Table 1) were sufficient to isolate the effects of the annual cycles of solar heating and SSTs. We have examined several diagnostics and simulation statistics to isolate the influence of the annual forcings on the annual and higher frequency modes of simulated circulation and rainfall.

Table 1. The Simulation Experiments

Simulations	NAME	Period	Starting day	Initial Soil Moisture	Surface Albedo and Vegetation Variations
Control; annual cycle Sun and SST.	C	50 mon.	First January	GSWP Analysis 1987	Annual cycle albedo Annual cycle vegetation
Annual mean Sun. Annual Cycle SST.	S1	50 mon.	First January	GSWP Analysis 1987	Annual mean albedo Annual mean vegetation
Annual mean SST. Annual Cycle Sun.	S2	50 mon.	First January	GSWP Analysis 1987	Annual cycle albedo Annual cycle vegetation
Annual mean Sun, and SST	S3	50 mon.	First January	GSWP Analysis 1987	Annual mean albedo Annual mean vegetation

4. Results.

Clearly, large changes are made to the solar and/or SST forcings, therefore we ignored the first two months of each model integration as an initial adjustment period for the simulated environment. Consequently, most of our analyses are based on the remaining 48 months or a subsequent period of four years. The internal dynamical variability is the only cause of interannual variability since both major external forcings are prescribed. Indeed, soil moisture is interactive in the simulation and that can introduce a systematic drift due to excessive drying or moistening. The Control run, C, plus three anomaly simulations S1 (without Solar annual cycle), S2 (without SST annual cycle), and S3 (without both the Solar and SST annual cycles) have been defined in section 3. June-July-August (JJA) and December-January-February (DJF) fields are analyzed to isolate the influence of the annual cycles of SST/solar forcings on global circulation and precipitation.

4.1 Time series of Zonal-mean Rainfall

Figure 3 shows the monthly zonal rainfall for each of the four simulations. The north-south excursions of the ITCZ for each of the four simulations: C, S1, S2, S3, can be seen in the top to bottom panels, respectively. The zonal excursions of the S1-ITCZ are relatively weaker as compared to C-ITCZ; however, as compared to S2, they are stronger in the tropics and weaker at the mid-latitudes, particularly, of the Northern Hemisphere, with more land-mass (Fig. 3c). Clearly, annual cycles of SST (Solar forcing) exert a significant influence on the ITCZ (surface fluxes and rainfall over high-latitudes land regions) both of which affect the zonal averages. Since both SST and land respond to the annual cycle of the solar radiation, while land area is only 30% of the ocean area, one might expect its influence to be about 30% of the total, which roughly holds in these comparisons. Thus SST annual cycle has a much stronger influence on the zonal excursion of the tropical ITCZ as well as the tropical rainfall even though ITCZ excursions do not correspond to monsoon excursions. In the higher latitudes, particularly in the Northern Hemisphere with larger land masses, the solar annual cycle produces a significant effect on the rainfall annual cycle. The ITCZ excursions are replaced by a flat broad ITCZ in S2. Case S3, with no annual cycle for the SST or solar flux would be expected to simulate a steady state response and indeed it does (Fig. 3d); the small interannual variability merely reflects non-linear internal dynamical influences, which are well within the expected limits.

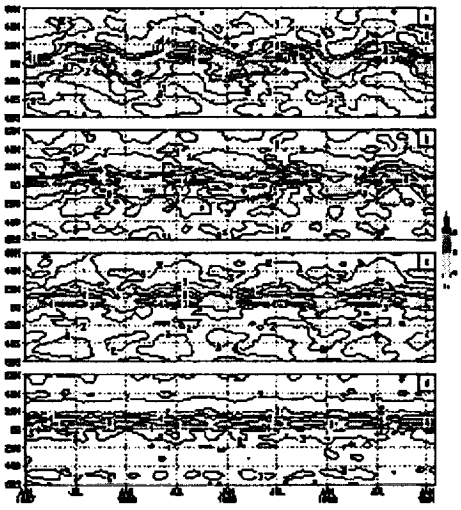

4.2 Precipitation

The four year JJA (DJF) precipitation fields are shown in Fig. 4 (Fig. 5). In accord with Figure 3a, the annual mean and summer ITCZ are well simulated in Control, C in Fig. 4a (Fig. 5a). The simulation S1 with no solar annual cycle (Fig. 5b) shows an ITCZ similar to that of C particularly across the tropical Pacific Ocean. However, the simulated rainfall over India and China increases (decreases) in response to the summer (annual mean) forcing of solar irradiance. In addition it is also larger over the warm pool region of tropical East Pacific. In contrast, the simulated JJA rainfall over tropical Africa increases (decreases) in S1 (S2) as compared to C. Summer solar irradiance produces intense heating of the Eurasian land masses, which can be expected to draw trade wind moisture transports into India. This could be viewed as thermally driven and

frictionally controlled moisture flux transport. Lacking strong summer solar heating, as is the case of the annual mean solar forcing simulation, S1, the moisture flux transport stays partly over the ocean and is partly diverted to Africa whereby the rainfall over tropical Africa increases (Fig. 5b). On the other hand, S2, with the full annual cycle of the solar forcing, but without the SST annual cycle, simulates relatively more rainfall over India and China and less over Africa as compared to S1 simulation. However, the key land features of S2 simulation are midway between S1 and C. This suggests that SST and solar annual cycles have a positive feedback effect on each other. In the third integration (not shown) called S3 without the annual cycle of SST and solar income, African rainfall was strong though somewhat to the south, while the Indian monsoon did not develop. If the model can be assumed to simulate the realistic scenarios, the summer solar heating of land, as would be implicit in the annual solar cycle, leads to copious (deficient) rainfall over India (Africa). Indeed, without such a heating of large land masses of the northern hemisphere, all major rainfall distribution centers tend to position themselves southwards. Particularly over India, the annual solar and SST cycle appear to work in concert for producing the simulated Indian monsoon.

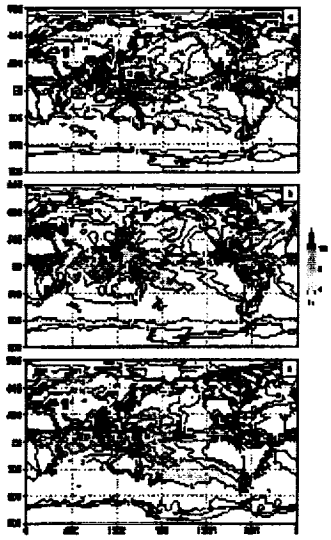

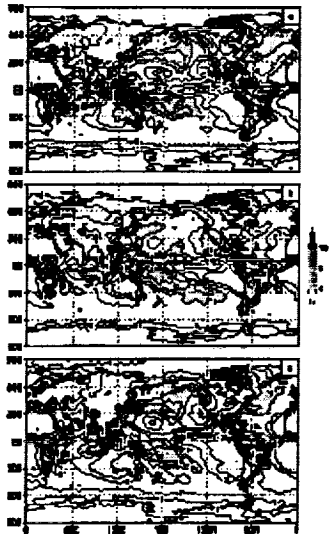

For boreal winter, DJF, we see that the Australian monsoon (Fig. 5a) also reveals some interesting characteristics of the combined influence of solar and SST forcings. Neither the SST annual cycle of S1 (Fig. 5b) nor the solar heating annual cycle of S2 (Fig. 5c) can produce the Australian monsoon when invoked in a stand-alone mode. Even when the two are added (not shown), they do not sum up to the Australian monsoon rainfall and circulation simulated by C (Fig. 5a). Here also the tropical African rainfall is strongest without the solar annual cycle. It is somewhat weaker, nevertheless stronger than that of C, for no SST annual cycle simulation. Over the Amazonia, the typical rainfall gets a typical 3-center structure in response to both the SST and solar annual cycles. The 4-6 mm/day rainfall over North Pacific gets substantially reduced (maximum of 4mm/day) in S1. In other words the results suggest that the rainfall structures are strongly linked to the solar annual cycle. We shall examine this further in section 4.6. There are other differences in ITCZ, SPCZ, and rainfall over the Himalayas and so on. For example, the Himalayan rainfall, which is attributed to winter time disturbances show a substantial decrease in the S1 simulation but without much change in the structure while it develops a somewhat different structure in S2.

4.3 Hadley Cells

Each of the four Hadley cells for boreal summer (JJA) shows a consistent response to the annual cycle of solar and/or SST forcings. The simulated Hadley cell is realistic as well as strongest in C (Fig. 6a). It gets significantly weaker in simulations without the solar annual cycle, S1 (Fig. 6b). In S2 without the SST annual cycle (Fig. 6c), the Hadley cell is much stronger than that of S1 but somewhat weaker than that of C. This suggests, boreal summer season solar heating of is imperative to the development of a strong Hadley cell. However, if both the SST and solar annual cycles were eliminated, the simulated Hadley Cell is the weakest among all the simulations (S3, Fig. 6d). For this reason, we argue that both the solar and SST annual cycles work in unison to produce the observed strength and structure of the Hadley Cell of JJA. The second equally interesting feature though is the Ferrel Cell of the Northern Hemisphere. In the absence of summer solar heating, particularly over land, the air at about 30 N (with large land-mass) cools and sinks to induce compensatory adiabatic warming that must make up for the deficit in solar heating and maintain the horizontal temperature gradients and vertical lapse rates. This is able to strengthen the indirect Ferrell Cell significantly (Fig. 6b &d) as seen in S1 and S3 simulations both of which lack the strong Boreal summer Sun. On the other hand, Figures (6 a & c) show that the solar annual cycle with strong heating of land masses of the Northern Hemisphere is primarily responsible for the observed structure of the Hadley cell. Figures (6c and d) show a relatively weaker Ferrell Cell in the Southern Hemisphere; both of these simulations use an annual mean SST. Since, there is a large ocean cover over the southern mid-latitudes, such an influence of SST on the meridional circulation is a natural consequence.

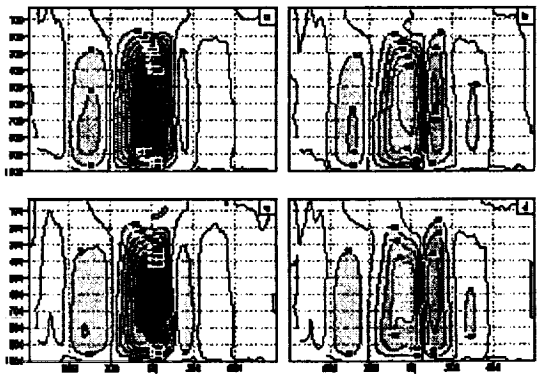

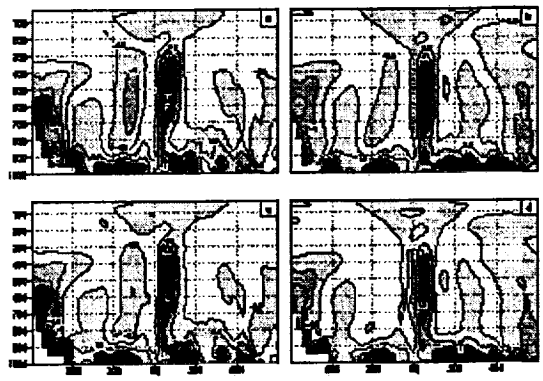

The corresponding diabatic heating (Fig. 7), which is the sum of radiative and condensation heating for JJA, shows how it relate to the mean meridional circulation depicted in Figure (6). First, Figure 7a and c are more similar to each other in the tropical region suggesting the importance of the JJA Sun for tropical diabatic heating. The annual mean solar forcing creates fall-like conditions for the southern (northern) high latitudes which implies more (less) sunshine than in JJA and less cooling (Fig. 7b and d) versus the winter-like solar forcing of C and S2 (Fig. 7a and c). The least diabatic heating occurs in the equatorial region of S3 (Figs. 7d) with no annual cycle of SST and solar flux; it corresponds with the weakest Hadley circulation (Fig. 6d). There are several other features like large differential heating or cooling at the polar latitudes in response to changes in the solar income between the annual versus JJA, but some such differences are self

evident and require no further elaboration. It may be pointed out, however, that the changes in the mean meridional circulation and diabatic heating structures are internally consistent and reasonably explainable. Similar features with 6-months phase, i.e., Northern hemisphere features replacing Southern Hemisphere features and vice versa, were noted for DJF and are not discussed here.

4.4 Indian Monsoon

Wet summers and dry winters type of climatology generally characterize Indian monsoons. The classical view has been that solar heating of land and the lower troposphere atop produces a thermal low (during boreal summers) that helps to establish the Indian monsoon. The water vapor transport and rising motion generated by the solar heating of the sub-continent supports moist convection, which in turn releases the latent heat of condensation to exert a positive feedback on the maintenance of the monsoon circulation and rainfall. The Indian monsoon positively feeds back on the trades that converge into India from the west replacing the local wintertime easterlies. The influence of the annual cycle of solar forcing and SSTs on the Indian monsoon is clearly demonstrated in JJA rainfall (Fig. 8). Without summer heating by the Sun, the four-year mean rainfall (Fig. 8a) is markedly reduced over the Indian subcontinent (simulation S1; Fig. 8b) as well as in S3 (not shown). The typical monsoon westerlies that usually emanate from the Indian Ocean into the Indian subcontinent do not develop in S1. In fact the entire monsoon circulation, except for westerly flow from 5S to 5N, is in disarray. Accordingly, there is very little rainfall over coastal Western India including the Ghats and there is no discernible summer monsoon in S1. Nevertheless, more rainfall accompanies the monsoon-like circulation over the equatorial Indian oceans. In simulation S2, with the annual cycle of solar forcing, i.e., JJA sunshine, the GCM is able to simulate discernible signatures of the Indian monsoon without the help of JJA SST (Fig. 8c). From these diagnostics, we infer that solar heating of the land masses of the Northern Hemisphere in the summer season is the primary driver of the Indian monsoon into land regions, which is a classical concept. If we look at the differences between the rainfall fields of Figures 8c and 8a, we note the relative unimportance of the SST annual cycle (not shown); indeed, it is much smaller than the corresponding solar annual cycle influence. Although both annual cycles, SST and solar, have a positive influence on the vitality of the simulated Indian monsoon, their respective importance is abundantly clear from our simulation studies. Without the intrinsic support of solar heating of land, the annual cycle of SST is not able to invigorate the Indian monsoon, while in S2, the JJA Sun helps significantly to simulate the overall monsoon circulation. We infer that it is the land heating of the summer Sun that draws the trade-wind moisture into the Indian subcontinent causing winds to change from easterly to westerly and bring about the onset of Indian Monsoon. On the other hand, the simulated tropical African rainfall is larger in S1. Lacking JJA solar forcing, the simulated tropical African rainfall increases while the Indian monsoon gets weaker- a result that could be evaluated in observational data by aggregating years in which Indian and African JJA rainfall shows the tell-tale signs of above relationship. These results are in general agreement with those of Shukla and Fennessy, (1994).

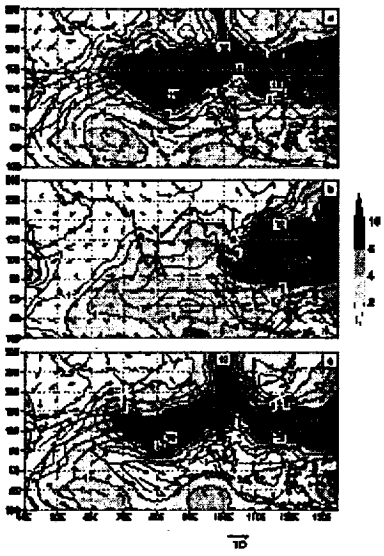

4.5 Rainfall in the Indian Longitudes

The rainfall over 65-90E, the longitude of the Indian subcontinent plus surrounding oceans of the region, is analyzed further by examining the zonal average rainfall time series for the region. The simulated annual cycles of precipitation for the three cases (C, S1 and S2), shows that in the summer the northward extension of the monsoon rainfall that engulfs the Indian subcontinent is clearly forced by solar heating of land (Fig. 9a and c). Figure 9a shows a sudden onset in mid-May; it maintenance till end of August and a slow withdrawal follows subsequently. It is similar to what has been well documented in the analysis of the rainfall observations. For the annual mean Sun, the annual cycle of rainfall does not have any development in the summer season (Fig. 9b). In simulations, C (Fig. 9a) and S2 (Fig. 9c) invoking the annual solar cycle, there is a distinct heavy precipitation between 5N - 20N during June-July-August around the latitude of the Indian land-mass. The simulation without the annual cycle of SST (Fig. 9c) shows, in addition, a distinct deficit in rainfall in the equatorial region, which is not found in either C or S1 (Figs. 9a & c, respectively). We naturally infer that lack of the SST annual cycle is the cause of this rainfall deficit. We compared the simulated vis-à-vis analyzed rainfall (not shown) and found that the model potentially does a reasonable job of simulating Indian monsoon rainfall. This gives us a reasonable confidence in the above inferences. Moreover, the rainfall at about 30N, which is evidenced in Figure 9a and 9c, is totally missing in Figure 9b. Thus Boreal summer sun not only is responsible for the Indian monsoon, but it affects rainfall over land even at 30N and beyond, a reasonably understandable inference.

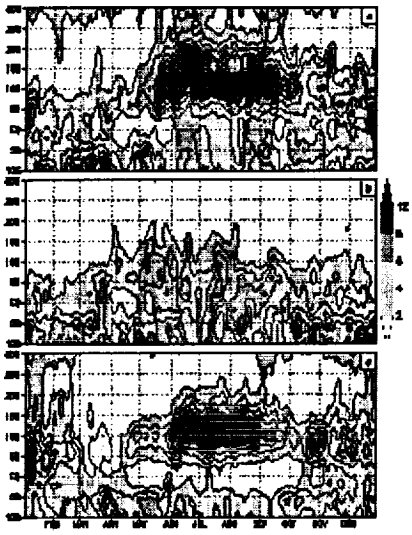

4.6 Annual Cycle of Precipitation

The structure of the annual cycle of precipitation can be discerned by Fourier decomposition of the rainfall at each grid point independently. Clearly, the first harmonic is the annual mode. The global distribution of this mode for the Control case, C (Fig. 10a), shows a JJA phase over India, China and large parts of south-east Asia representing (Boreal) summer monsoons. We also see a summer (winter) mode over northern (southern) Africa. There are some equally strong annual modes of precipitation over the Indian, Pacific, and Atlantic oceans. Figure (10a) reveals their relative phases and strengths. Warm water of the Gulf (east coast of North America, everywhere) regions produce a Boreal winter mode, while North and South Pacific regions have some very strong modes that reverse phases over a short distance. In the ITCZ region (100W to 175W), the phases of precipitation to the north and south of the ITCZ merely reflect the 6-month out-of-phase relationship of the ITCZ in the Boreal summer and winter. The Eastern Pacific annual mode shows a gradual advance in the phase of the summer mode (extending to September) as we go northwards from the equator; the case for the southern Eastern Pacific is quite the opposite, but there are some significant differences among them. We submit, these phase changes are reflections of the movement of the land-ITCZ of the tropical Pacific into northern (southern) latitudes in boreal summer (winter) seasons.

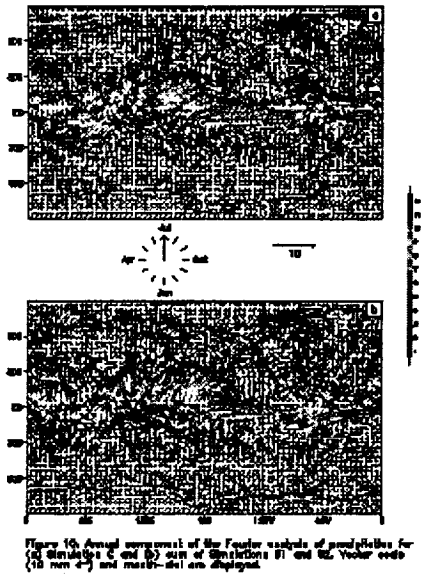

The annual mode of rainfall simulations simulated by S1 (Fig. 11a) and S2 (Fig. 11b) show a very interesting story. First, the annual precipitation mode over Amazonia has a month of April phase in the tropical region and a month of January phase southward of the equator (Fig 10a). Simulation S1, with annual cycle of SST, shows the month-of-April mode in the tropical region (Fig. 11a), whereas simulation S2 with only the annual cycle of solar forcing shows the month-of-January/February mode mostly in regions southward of the equator (Fig. 11b). The sum of these two phases (Fig. 10b) reveals a pattern and strength similar to that of Control case C (Fig. 10a). Thus simulation C represents a scenario, which exhibits the combined effects of both modes. These modes explain up to 70% of the annual rainfall variability particularly in the tropics. The annual rainfall modes (Fig. 10a) in the Northern Pacific regions are also reproduced by the sum of S1 and S2 modes while S1 has a month of September phase and S2 has a month-of-July phase. This shows that solar forcing in the summer season contributes to a strong phase of annual cycle of precipitation in the northern regions of Eastern Pacific. Both over India and Australia, the monsoon in C is much stronger than the monsoon in either S1 or S2 or even the sum of the S1 and S2. This suggests that strong monsoon circulation and rainfall is due to the combined influence of the solar and SST forcings in the respective monsoon season. However, weaker monsoon precipitation over India is accompanied by a stronger monsoon over tropical Africa as was discussed earlier.

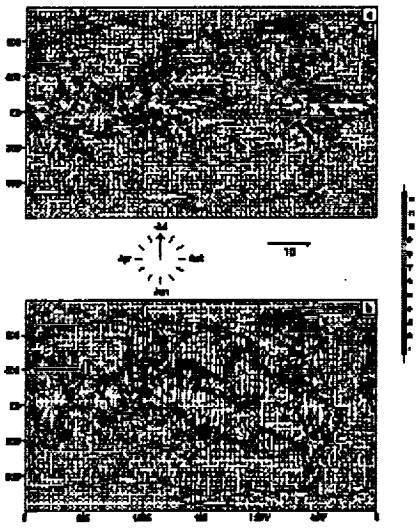

4.7 Tropical Intraseasonal Oscillation

One of the crucial features affecting tropical circulation and rainfall, even the onset of Asian monsoons is the 30-60 day mode; it is often called tropical intraseasonal oscillation (TIO). We had simulated them well in the earlier version of our GCM, called GLA GCM. Indeed, our current GEOS 2 GCM with McRAS (uses RAS as a cumulus convection scheme) also simulates them well although they are somewhat weaker. An outstanding observation of Figure 12 is that TIOs are equally well simulated with or without the annual cycle of the solar insolation or SST. This result suggests that TIO are an internal mode of the atmospheric dynamics and time-scales associated with physical processes. It does not depend much on the annual cycle of SST or the annual cycle of solar heating that manifests through earth's surface fluxes. Indeed, TIOs have a natural vacillation and are known to be stronger in winter- a scenario identifiable in C; they are also discernible somewhat in the simulation with only the annual cycle of SST, (simulation S1), but TIOs are unremarkable in simulations S2 and S3 in which SST annual cycle is absent. This suggests that stronger TIOs in winter may be forced by seasonal changes in SST. A more detailed investigation of these issues is beyond the purview of the current study, but could be the subject of a future investigation.

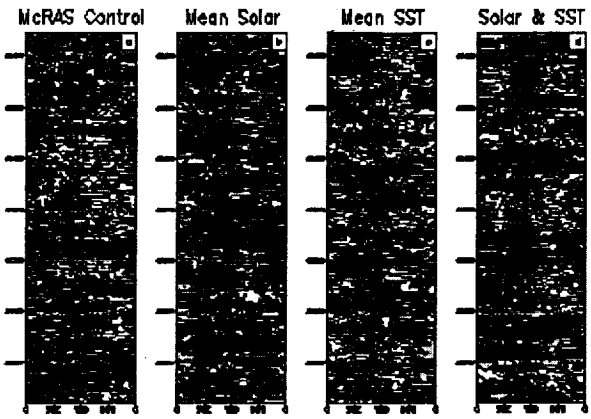

4.8 Diabatic Heating and Moisture Transports

The column-mean moisture transports and convergences (Fig. 13) are much less alike for C (S1) simulation with annual cycle (mean) Solar flux (panels a vis a vis b) as opposed to C and S2 simulation (panels a *vis-a-vis* c). We note Indian monsoon, tropical African circulation, South American flows are closer to each other in Figs. 13a and 13c. Although SPCZ and in southern high latitudes are very similar in all runs, the climatologies of northern Atlantic and Pacific are again better simulated in the annual mean SST simulation, S2, but with the solar annual cycle. These simulations again show that the solar heating during the summer seasons is primarily responsible for the peculiar structure of the global patterns of rainfall and diabatic heating. As pointed out earlier, both SSTs and summer solar heating have a role in the vitality of the Indian as well as Australian monsoons. Nevertheless, a comparison of the three panels, a b & c, of Figure 10 clearly shows that the solar heating of land masses and its dependent structures of circulation are the dominant driver of the Indian and Australian monsoons.

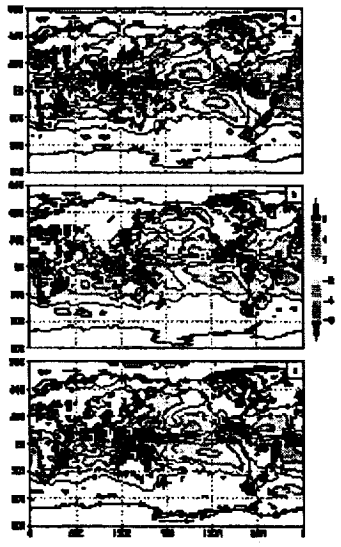

4.9 Pentad Precipitation History for India

The pentads of northward march of Indian monsoon from the month of May through September were examined. Indian and nearby Indian Ocean simulated rainfall for five months: May-June-July-August-September, are shown for each of the four cases: C, S1, S2, S3 in Figures (14a, b, and c). In the Control, C, the Indian monsoon, which is at about 10N in the beginning of May, evolves to engulf the entire subcontinent by mid-June, a scenario which is well documented in the observations and is also evident in the DAO-DAS analyzed data product. Our simulation uses climatological SSTs while DAO-DAS was forced with SSTs from NCEP Analysis, so some differences are bound to emerge. Nevertheless, our plots depict averaged rainfall and circulation for the 4-year period starting from January 1, of the first year "arbitrarily called 1987 in C". The monsoon in C withdraws around the third week of September whereas in the DAO analysis the rains over Indian subcontinent persist till the first week of October. Both answers are plausible; however, we must recognize that our Control with climatological SSTs is not a nature run and therefore it can't be truly compared with the DAO-DAS data products. The main purpose of comparing and analyzing these rainfall patterns is to determine if the model simulates a respectable onset and withdrawal of monsoon, which was evident in Fig 14a. In contrast, there is virtually no monsoon onset or development in the annual mean solar flux simulation, Fig. 14b. On the other hand, the annual mean SST simulation (Fig. 14c), has a sudden monsoon-like onset and withdrawal, even though it is somewhat delayed and much weaker. The GEOS DAS has a much earlier onset of monsoon, which is much stronger and longer lasting. Clearly, GEOS DAS monsoon data is at significant variance with the current GEOS GCM simulation as well as documented observations; however, the key point to emphasize is that the climate version of GEOS GCM simulates a more realistic character of Indian monsoon. This potentially gives us confidence in the reliability of our simulation studies and the key inferences.

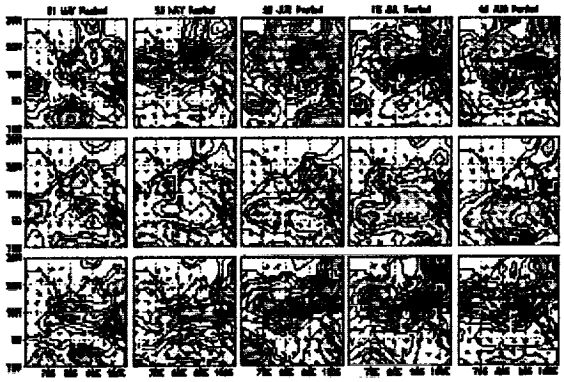

5. Discussions and Conclusion

A climate version of GEOS 2 GCM that contains important new upgrades to model's prognostic clouds, cloud microphysics, and snow and ice hydrology was used to isolate the influences of the annual cycles of solar irradiation and sea-surface temperatures (SSTs) on the simulated circulation and rainfall. The scientific motivation for comparing two experimental simulations, one with the

annual mean SST and one with annual mean solar flux at the top of the atmosphere, with the Control and DAO-DAS data, was to isolate how these forcings affect the tropical rainfall and circulation. Four 4-year long integrations: C, S1, S2, and S3, were generated with the GCM. We point out that these simulations are not nature runs, but are used merely to discern how the two annual cycles interact with each other? Secondly, the objective was to find out whether we could learn something by isolating these influences? These goals have been adequately accomplished within the limitations of the GCM used for the study. However, because the GEOS 2 GCM is a remarkably credible state-of-the-art climate system model, we submit that these limitations do not materially impair our findings. The nature run, C, and its comparisons with the annual mean solar forcing simulation, S1, and the annual mean SST simulation S2 and the joint annual mean SST and solar forcing simulation, S3, reveal the following:

1. The 30-60 day oscillations (also called tropical Intraseasonal Oscillations or TIOs) are equally well simulated in each of the four integrations except for a miniscule hint that the vigor of TIOs in winter may be related to the annual cycle of SSTs. These simulations suggest that TIOs are largely a by-product of the internal dynamics of the atmosphere produced by robust physical processes of the atmosphere and are weakly linked to the annual cycles of heating or cooling as manifested by the annual cycles of land temperatures or SSTs. This conclusion is also borne out by the behavior and persistence of TIOs, which holds robust through out the year despite being somewhat stronger during boreal winters.
2. The northward excursion of the monsoon into the Indian subcontinent in Boreal summer periods is very much modulated by the SST annual cycle, but in contrast it is predominantly governed by the solar annual cycle. Our simulations show that the Indian summer monsoon is relatively stronger (weaker) in S2 (S1) invoking the realistic annual cycle of solar heating (SSTs) along with annual mean SST (solar income). Without the local summer solar heating, both Indian and Australian monsoons do not develop and without the annual cycle of the SSTs, they both do not emerge as strong.
3. The rainfall over Amazonia produces regions with (i) a strong phase for the month of March in the tropics for the SST annual cycle simulation and (ii) a strong phase for the month of January polewards of the tropics for the solar annual cycle. It is interesting to note that the Control C, which has both annual cycles, exhibits a combination of both annual cycles. We argue, these phases of the annual rainfall over Amazonia are determined by the annual cycles of SST and solar flux working in concert particularly in the South American region.
4. We show that the Boreal summer rainfall in Sahelian Africa is significantly reduced lacking increased solar heating of the Northern Hemispheric land masses. This holds good for all monsoonal regions: India, South-East Asia, as well as Australia. The only exception is the Continental United States, where the two annual cycles: SST or Solar forcing of the Earth system which is predominantly through land masses and all atmospheric airmass, show relatively marginal effects.
5. The stationary circulation patterns over the vast land masses of the Northern Hemisphere at mid and high latitudes gets strongly influenced by annual cycle of solar heating. In fact there was a hint that the solar income changes set up a wave train type of circulation anomaly patterns. Therefore we infer that solar forcing strongly affects the circulation over vast land masses of the Northern Hemisphere in the Boreal summer season which has been analyzed in these comparisons.
6. The circulation patterns over the Kuroshio currents off the East Coast of Asia get affected far more in S2 as compared to S1 or S3. Since gulf stream and its annual cycle is directly involved, we infer that these circulation and rainfall patterns are strongly linked to the SST naturally giving importance to the annual cycle of SSTs.

Acknowledgments: This simulation study evolved into a full investigation serendipitously. Nevertheless, the funding support of our simulation studies research by NASA headquarters under GMAP program helped participation of G. K. Walker. Vikram Mehta support under Oceanography helped his participation.

References

Arakawa, A. and W. H. Schubert, 1974: Interaction of a cumulus ensemble with the large-scale environment, Part I. *J. Atmos. Sci.*, **31**, 674-701.

Cheng, M.-D., 1989: Effects of downdrafts and mesoscale convective organization on the heat and moisture budgets of tropical cloud clusters. Part I: A diagnostic cumulus ensemble model. *J. Atmos. Sci.*, **46**, 1517-1538.

Chandrasekar A, Kitoh A, 1998: Impact of localized sea surface temperature anomalies over the equatorial Indian ocean on the Indian summer monsoon. *Journal of the Meteorological Society of Japan* **76**: (6) 841-853.

Cahalan, R., 1994: Bounded Cascade Clouds: albedo and effective thickness. *Non-linear Processes in Geophys.*, **1**, 156-167.

Chou, M.-D., and M. J. Suarez, 1994: An efficient thermal infrared radiation parameterization for use in general circulation models. *NASA Technical Memorandum* **104606**, 3, 85 pp. NTIS# N95-15745.

Chou, M.-D., M. J. Suarez, C.-H. Ho, M.-H. Yan, K.-T. Lee, 1998a: Parameterization for cloud overlapping and shortwave single scattering properties for use in general circulation and cloud ensemble models. *Jour. of Climate*, **11**, 202-214.

Chou, M.-D., K.-T. Lee, S.-C. Tsay, and Q. Fu, 1998b: Parameterization of cloud longwave scattering for use in atmospheric models. *Jour. of Climate*, (in print).

Del Genio, A. D., N.-S. Yao, W. Kovari, and K. K.-W. Lo, 1996: A prognostic cloud water parameterization for general circulation models. *J. Climate*, **9**, 270-304.

Gadgil S, Sajani S, 1998: Monsoon precipitation in the AMIP runs. *Climate Dynamics* **14**: (9) 659-689.

Gadgil, S., 2000: Monsoon-ocean coupling. *Current Science* **78**: (3) 309-322.

Hahmann, A. N., and R. E. Dickinson, 1997: RCCM2-BATS model over tropical South America: Application to tropical deforestation. *J. Climate*, **10**, 8, 1944-1964.

Helfand, M. H., and J. C. Lebraga, 1988: Design of a non-singular level 2.5 second order

closure model for prediction of atmospheric turbulence. J. Atmos. Sci., **45**, 113-132.

Krishnamurti, T. N., Kishtawal C. M., 2000: A pronounced continental scale diurnal mode of the Asian summer monsoon. *Mon. Wea. Rev.* **128**, 462-473.

Lohmann, U., N. McFarlane, L. Levkov, and K. Abdella, 1998: Comparing different cloud schemes of a single column model by using meso-scale forcing and nudging technique. *J. Climate*, **12**, 438-461.

Lau K. M. and P. H. Chan, 1986: Aspects of the 40-50 day oscillation during the northern summer as inferred from outgoing longwave radiation. *Mon. Wea. Rev.*, **114,** 1354-1367.

Mocko, D. M., and Y. C. Sud, 1998: Comparison of land surface model (SSiB) to three parameterizations of evapotranspiration-a study based on the ISLSCP Initiative I data. *Earth Interactions,***2**, 40pp.

Mocko, D. M., and Y. C. Sud, 2001: Further refinements to the snow-physics scheme for use in SSiB using GSWP and Valdai data (*Earth Interactions, to Appear*).

Ogasawara N, Kitoh A, Yasunari T, Noda, 1999: Tropospheric biennial oscillation of ENSO-monsoon system in the MRI coupled GCM. *Journal of the Meteorological Society of Japan 77:* (6) 1247-1270.

Ou , S. C., and K. N. Liou, 1995: Ice microphysics and climate temperature feedback. *Atmos. Res.* **35**, 127-138.

Mandke S. K., Soman M.K., Satyan V., 1999: Impact of convective downdrafts in a GCM on the simulated mean Indian Summer Monsoon and its variability. *Journal of the Meteorological Society of Japan* **77**: (5) 1061-1082.

Moorthi, S., and M. J. Suarez, 1992: Relaxed Arakawa-Schubert: A parameterization of moist convection for general circulation models. Mon. Wea. Rev. **120**, 978-1002.

Shukla, J. and M. J. Fennessy, 1994: Simulation and predictability of monsoons. Proceedings MONEG International Conference on Monsoon Variability and Prediction, Trieste,

Slingo, J., 1987: The development and verification of a cloud prediction scheme for the ECMWF model. *Quart. Jour. Roy. Met. Soc.*, **106**, 747-770.

Suarez, M. J., and L. L. Takacs, 1995: Documentation of Aires/GEOS dynamical core version 2, *NASA Tech. Memo. **104606***, Vol. 5, Goddard Space Flight Center, Greenbelt, MD 20771, 44 pp.

Sundqvist, H., 1988: Parameterization of condensation and associated clouds in models for weather prediction and general circulation simulation. In*: Physically based modelling and simulation of climate and climatic change,* (ed. M. E. Schlesinger), Riedel, Dordrecht, **Part 1**, 433-461.

Sud, Y. C., and G. K. Walker, 1993: A rain-evaporation and downdraft parameterization to complement a cumulus updraft scheme and its evaluation using GATE data. *Mon. Wea. Rev.,**11**, 3019-3039.*

_____, and G. K. Walker, 1999a: Microphysics of Clouds with the relaxed Arakawa-Schubert Scheme (McRAS). Part I Design and Evaluation with GATE Phase III data. *J. Atmos. Sci.,* **56**, 18, 3196-3220.

_____, and G. K. Walker, 1999b: Microphysics of Clouds with the relaxed Arakawa-Schubert Scheme (McRAS). Part II Implementation and Performance in GEOS 2 GCM. *J. Atmos. Sci.,***56**, 18, 3121-3240.

Torrence C, Webster P. J., 1999: Interdecadal changes in the ENSO-monsoon system. *Journal of Climate***12**: (8) 2679-2690, Part 2 Aug. 1999.

Wang H. J , 2000: The interannual variability of East Asian monsoon and its relationship with SST in a coupled atmosphere-ocean-land climate model. *Advances in Atmospheric Sciences***17**: (1) 31-47.

Webster, P. J., V. O. Magana, T. N. Palmer, J. Shukla, R. A. Tomas,, M. Yanai, and T. Yasunari, 1998: Monsoon: Processes, predictability, and the prospects for prediction. *J. Geophys. Res.,* **103**, 14,451-14,510.

Yang, S., and K. M. Lau, 1998: Influence of SST and Ground Wetness on the Asian Summer Monsoon. *J. Climate,***11**, 3230-3246.

Zhou, J., Y. C. Sud, K.-M. Lau, 1996: Impact of orographically induced gravity wave drag in the GLA GCM. Quart. J. Roy. Met. Soc., **122**, 903-927.

Figure Legends

Figure 1. Annual cycle of Zonal mean incoming solar radiation in Wm^{-2}. The lines on the right hand panel show summer (JJA), winter (DJF), and annual mean values

Figure 2. 30-year Sea-surface Temperature (SST) climatology (a) annual mean, (b) summer (JJA) minus annual mean, and (c) winter (DJF) minus annual mean in deg. C.

Figure 3 Zonal monthly precipitation (mm d^{-1}) for four 50 month integrations. (a) Control, C; (b) Simulation S1 with incoming solar held at annual mean, (c) Simulation S2 with SST held at annual mean, (d) Simulation S3 with both incoming solar and SST held constant at annual mean value.

Figure 4. Summer (JJA) precipitation as a mean of the 4-year simulation for (a) Simulation C, (b) Simulation S1 and (c) Simulation S2. Contours are drawn for 1, 2, 4, 6, 8, 12, and 16 in mm d^{-1}.

Figure 5 Same as Fig.4 except for winter (DJF).

Figure 6. Summer (JJA) Hadley Circulation (10^9 kg sec^{-1}) for the 4-year mean model integration for (a) Simulation C, (b) Simulation S1, (c) Simulation S2, and (d) Simulation S3.

Figure 7. Summer (JJA) diabatic heating (K d^{-1}) for the 4-year mean model integration for (a) Simulation C, (b) Simulation S1, (c) Simulation S2, and (d) Simulation S3.

Figure 8. Summer (JJA) precipitation (mm d^{-1}) and 850 hPa winds as a mean of the 4-year simulation for (a) Simulation C, (b) Simulation S1 and (c) Simulation S2. Contours are drawn for 1, 2, 4, 6, 8, 12, and 16 in mm d^{-1}. Color contrasts are chosen to discern the pattern differences. .

Figure 9. Patterns of 5-day running mean of precipitation (mm d^{-1}) averaged for Indian (65-90E) sector for (a) Simulation C, (b) Simulation S1 and (c) Simulation S2.

Figure 10. Annual component of the Fourier Analysis of precipitation for (a) Simulation C, (b) Sum of simulations S1 plus S2. Vector scale (10 mm d^{-1}), and month-dial are displayed.

Figure 11. Annual component of the Fourier Analysis of precipitation for (a) Simulation S1, and (b) Simulations S2. Vector scale month-dial are same as Fig. 11.

Figure 12 200hPa velocity potentials averaged for 10N-10S and 20-100 day band passed through Lanczos filtered for (a) Simulation C, (b) Simulation S1, (c) Simulation S2, and (d) Simulation S3.

Figure 13. Summer (JJA) precipitation minus Evaperation as a mean of the 4-year simulation for (a) Simulation C, (b) Simulation S1 and (c) Simulation S2. Contours are drawn for 1, 2, 4, 6, 8, 12, and 16 in mm d^{-1}. Color bar shows the pattern demarcations.

Figure 14. Summer (JJA) pentad precipitation patterns for the 4-year mean simulation over the Indian sector for (a) Simulation C, (b) Simulation S1 and (c) Simulation S2. Contours are drawn for 1, 2, 4, 6, 8, 12, and 16 in mm d^{-1}. Color bar shows the pattern demarcations.